Materials Characterization 113 (2016) 82–89

Contents lists available at ScienceDirect

Materials Characterization

journal homepage: www.elsevier.com/locate/matchar

Structural and mechanical characterization of boron doped biphasic calcium phosphate produced by wet chemical method and subsequent thermal treatment

Onder Albayrak

Department of Mechanical Engineering, Faculty of Engineering, Mersin University, Yenisehir, 33343, Mersin, Turkey

ARTICLE INFO

Article history:
Received 11 November 2015
Received in revised form 8 January 2016
Accepted 9 January 2016
Available online 12 January 2016

Keywords:
Boron doped hydroxyapatite
Tricalcium phosphate
Biphasic
Calcium phosphate
Synthesis
Sintering

ABSTRACT

In the current study, boron doped biphasic calcium phosphate bioceramics consisting of a mixture of boron doped hydroxyapatite (BHA) and beta tricalcium phosphate (β-TCP) of varying BHA/β-TCP ratios were obtained after sintering stage. The effects of varying boron contents and different sintering temperatures on the BHA/β-TCP ratios and on the sinterability of the final products were investigated. Particle sizes and morphologies of the obtained precipitates were determined using SEM. XRD and FTIR investigation were conducted to detect the boron formation in the structure of HA and quantitative analysis was performed to determine the BHA/β-TCP ratio before and after sintering stage. In order to determine the sinterability of the obtained powders, pellets were prepared and sintered; the rates of densification were calculated and obtained results were correlated by SEM images. Also Vickers microhardness values of the sintered samples were determined. The experimental results verified that boron doped hydroxyapatite powders were obtained after sintering stage and the structure consists of a mixture of BHA and β-TCP. As the boron content used in the precipitation stage increases, β-TCP content of the BHA/β-TCP ratio increases but sinterability, density and microhardness deteriorate. As the sintering temperature increases, β-TCP content, density and microhardness of the samples increase and sinterability improves.

1. Introduction

Hydroxyapatite (HA) and beta tricalcium phosphate (β-TCP) have been extensively used in medical and dental applications [1] since "HA exhibits strong affinity to host bone tissues because of its close similarity in chemical composition with natural bone and its high biocompatibility" [2,3] and "β-TCP is proved to be resorbable in vivo with promoting bone growth to the implanted β-TCP" [2]. In spite of the stated advantages of HA and β-TCP, there are some limitations of these bioceramics. Low resorption of HA within the body obstructs the formation of new bones into the implant and bone remodeling; moreover since only a limited amount of HA is replaced with bone, local instability and stress concentrations arise [1,4]. On the other hand, absorption rate of β-TCP does not allow required time to bone ingrowth, resulting in insufficient bone replacement [1,5]; moreover β-TCP lacks osteogenic property [1,6]. In order to overcome or decrease these types of deficiencies of single HA and single β-TCP, there is a growing interest in developing HA/β-TCP biphasic calcium phosphate (BCP) ceramics [7].

BCP bioceramics, consisting of a mixture of HA and β-TCP of varying HA/β-TCP ratios, are more effective in bone repair and bone regeneration than pure HA or pure β-TCP [7], and have the benefits of combining the stability of HA with the reactivity of β-TCP [8]. The concept is to obtain a balance of the more stable phase of HA and more soluble phase of β-TCP [9] and to control the degradation rate to a certain degree [7,10]. This situation encourages the bone remodeling and new bone formation by allowing bone ingrowth as partial dissolution of BCP releases calcium and phosphate ions in the local environment [9,11]. In-vitro and in-vivo tests conducted on the BCP granulates with the specific content of 62% HA and 38% β-TCP indicated that BCP granulates have no cytotoxic effects on MG-63 cells, show good biocompatibility and provide a strong positive effect on bone regeneration [12].

These mentioned advantages of BCP can be improved by doping the material with foreign elements. Boron is one of the promising foreign elements which is used for doping because of its positive effect on bone formation [13–15] and its possible antibacterial effect [16,17]. Jain et al. [13] mentioned that boron has beneficial effect on bone cell differentiation when added to bioglass bone-replacement scaffolds. Hakki et al. [14] mentioned that molecular level B has an important role on bone metabolism and may find novel usage at the regenerative medicine; furthermore Gorustovich et al. [15] stated that boron addition to 45S5 bioactive glass has positive effect on enhancing bone formation. Xue et al. [16] and Wang et al. [17] mentioned that boron doping to titania enhanced antibacterial efficiency compared with non-doped titania.

Abbreviations: B, Boron; HA, hydroxyapatite; BHA, boron doped hydroxyapatite; β-TCP, beta tricalcium phosphate; BCP, biphasic calcium phosphate.

E-mail address: albayrakonder@mersin.edu.tr.

http://dx.doi.org/10.1016/j.matchar.2016.01.006
1044-5803/

In literature, there is limited number of studies on the subject of boron doping to HA. In the study of Ternane et al. [18] calcium borohydroxyapatite was obtained by the solid-state reaction of $CaCO_3$, $(NH4)_2HPO_4$ and H_3BO_3 and subsequent heat treatment. They mentioned that the ratio of P/B affects the final structure; when the ratio is equal to 7.22 boron atoms will totally be introduced into the matrix lattice, however if the ratio is greater than 11, $Ca(OH)_2$ will be observed besides borohydroxyapatite and if the ratio is below 7.22, $Ca_3(BO_3)_2$ will also be observed [18]. Barheine et al. [19] prepared calcium borohydroxyapatite by the high temperature solid-state reaction of $CaCO_3$, $Ca_2P_2O_7$ and B_2O_3. They reported that besides the primary HA phase trace amounts of CaO and α-TCP were observed in the XRD spectra and BO_3, BO_2 and B–O groups were observed in the FTIR spectra [19]. When boron is added to the structure, borate groups would partially replace the PO_4 and OH groups [18–21]. Guler et al. [22] obtained calcium borohydroxyapatite without any other phases by the solid-state reaction using the starting materials $Ca_2B_6O_{11}\cdot 5H_2O$ and $(NH_4)_2HPO_4$, and applying a sintering step at 1200 °C for 12 h. Although they indicated that BO_3 would partially substitute the PO_4 groups, they did not observe any BO_2 groups in the FTIR spectrum [22]. Hayakawa et al. [23] synthesized boron-containing HA particles by using wet chemical method and subsequent heat treatment process. They stated that the chemical reaction between HA and $B(OH)_3$ has taken place above 900 °C [23].

To the best of knowledge of the author, the present work is the first study to obtain boron doped biphasic calcium phosphate bioceramics. In order to combine the advantages of boron and BCP, boron doped BCP bioceramics consisting of a mixture of boron doped hydroxyapatite (BHA) and TCP was produced in the present work. Boron doped BCP bioceramics with varying BHA/TCP ratios were obtained by using the wet precipitation method and then sintering consecutively. The effects of the boron contents used in the precipitation stage and the effects of sintering temperatures on the BHA/TCP ratios, densification, sinterability and microhardness of the final products were investigated.

2. Experimental

2.1. Production of powders and pellets

In this study, acid–base method was performed to synthesize non-doped HA powders since the reaction involves no foreign elements and the only by-product is water [2,24]. In this method, calcium hydroxide, $Ca(OH)_2$, and phosphoric acid, H_3PO_4 were used as Ca and P source, respectively, based on the following reaction:

$$10Ca(OH)_2 + 6H_3PO_4 \rightarrow Ca_{10}(PO_4)_6(OH)_2 + 18H_2O.$$

10.00 g of $Ca(OH)_2$ powder (~99%, Merck, Germany) was dissolved in 400 ml of deionized water at 40 °C using a magnetic stirrer for 30 min. 9.242 g of H_3PO_4 (85%, Merck, Germany) was added slowly at a rate of about 0.5 g/min to the continuously stirring $Ca(OH)_2$ solution to obtain of the stoichiometric Ca/P ratio of 1.67. After H_3PO_4 addition, the reaction mixture was aged at 40 °C for 48 h while stirring. Aged suspension of HA particles was centrifuged at 3000 rpm for 4 min, supernatant liquid was decanted and then precipitates were resuspended in 400 ml of deionized water. After this step was applied 5 times, the obtained

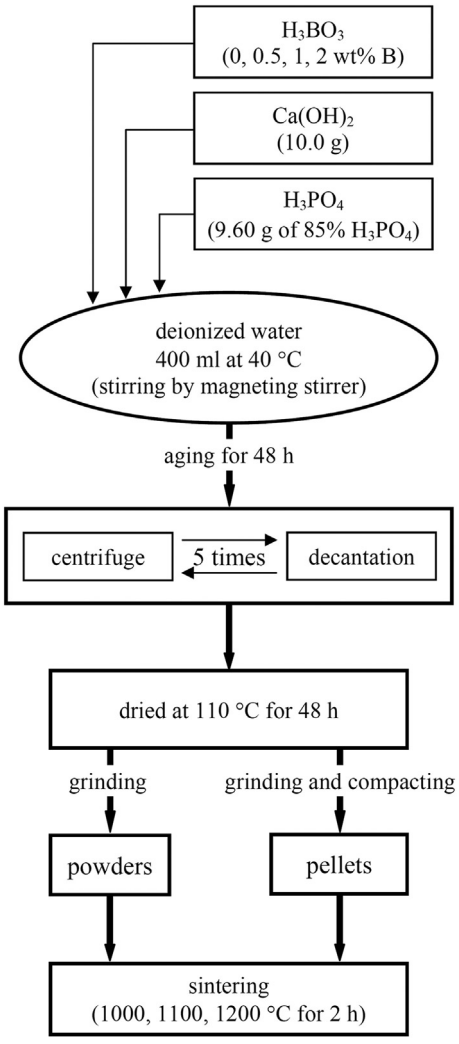

Fig. 1. Flowchart depicting the procedure to obtain undoped and boron doped BCP bioceramics.

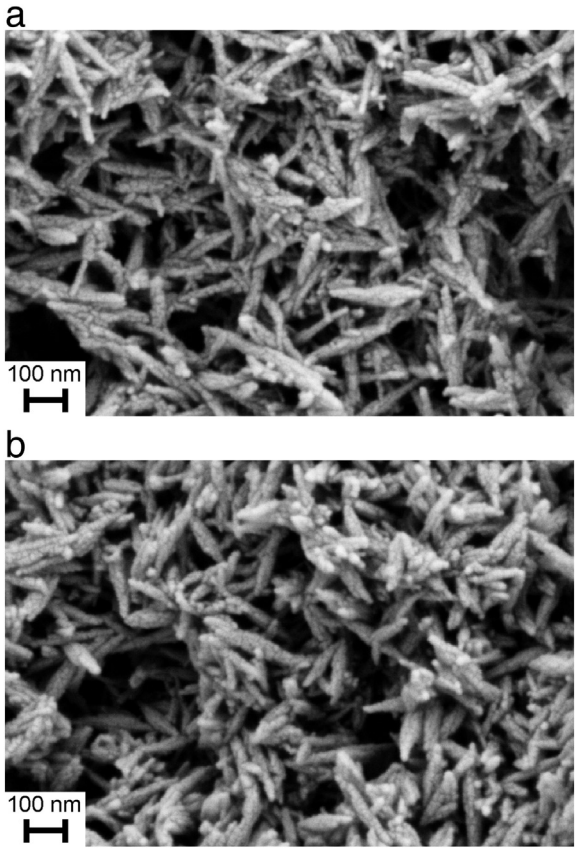

Fig. 2. FESEM micrographs (equal magnification) of synthesized powders at 40 °C for 48 h: (a) control sample (0 wt.% B addition), (b) 0.5 wt.% B addition.

precipitates were oven-dried at 110 °C for 48 h and grinded by hand for 10 min using an agate mortar and pestle.

As mentioned by Wei [25] and Tagai et al. [26], the chemical reaction provided above has been used to produce HA with the pH level kept above 9.50. Wei [25] and Tagai et al. [26] stated that great attention is required to keep the pH value of the synthesis solution above 9.5 if the aim is to obtain thermally stable HA powder because "if the pH value of the solution drops below 9, substantial amounts of β-TCP are formed" [25]. Kumta et al. [27] pointed out that adjusting the pH level of the synthesis solution above 10 is required to initiate the formation of stoichiometric and stable HA. Although HA powder could be obtained after synthesis even with a pH level below 9.5 as mentioned in [28], some portion of these HA powder decomposes after sintering and TCP occurs as a second phase which denotes that a synthesis pH below 9.5 results in HA which is thermally unstable. Therefore, in the process of HA synthesis by this reaction, usually ammonia or NH_4OH has been used to keep the pH value above 9.5 [29,30]. However, since the aim of the current study is to obtain boron doped BCP powders, the pH value of the synthesis solution which lies in the range of 7.10–7.40 is not changed in order to investigate the effects of the boron content and the sintering temperature on the structural and mechanical properties of the undoped and boron doped BCP samples.

The procedure used to synthesize boron doped HA powders is similar to the procedure described above. The only difference is the addition of H_3BO_3 as B source to the solution. Before $Ca(OH)_2$ addition, defined contents of H_3BO_3 powder (99.5%, Merck, Germany) were dissolved in 400 ml of deionized water to get 0.5, 1 and 2 wt.% B on the reactants side of the reaction.

In order to investigate the effects of B content and sintering temperature on the phase stability, phase purity and constitution, half of the green powders synthesized with different B contents such as 0, 0.5, 1 and 2 wt.% were sintered at 1000, 1100 and 1200 °C for 2 h.

The other half of the synthesized powders were compacted using a uniaxial press (MSE, MP10, Turkey) into cylindrical specimen with 10 mm diameter in a stainless steel die applying a pressure of 100 MPa for 90 s. Pelleted samples were sintered using the same conditions applied to the green powders and then the effects of both the B contents and the sintering temperatures on density and microstructure were investigated.

All the procedure mentioned in this section are illustrated step by step in the flowchart (Fig. 1).

2.2. Characterization

Morphology and particle size of the synthesized samples were observed by field emission scanning electron microscopy (FESEM) (Zeiss, Supra 55, Germany). Late in the precipitation process, 20 ml of sample was taken from the last resuspension solution. To remove the water stepwise 20 ml ethanol was added to the taken solution and the supernatant liquid was decanted after 15 min. The same resuspension and decantation process was applied further to obtain 25–75 and 0–100 vol% water–ethanol suspension to prepare the samples suspended completely in 100% ethanol stepwise for further SEM processing. Small amounts of this final suspension were dropped on top of the double stick carbon tape mounted on an aluminum stub. After drying at 40 °C for 12 h, all the samples were sputter coated (Quorum, UK) with platinum prior to FESEM examination to minimize any possible charging effects.

Phase identification, stability and constitution of the synthesized powders before and after sintering stage were investigated by powder X-ray diffractometry (XRD) (Model SmartLab, Rigaku, Japan). The XRD data were collected at room temperature over the 2θ range of 10°–70° at a step size of 0.02° and a scan rate of 5°/min. To determine the phases present, the obtained data were compared with the Joint Conference of Powder Diffraction (JCPDS) database. In addition to this, the weight ratios of the formed phases were quantified by the X-ray powder diffraction software package (PDXL 2.1, Rigaku, Japan) using Rietveld analysis [31].

Fourier transform infrared (FTIR) spectroscopy (Model FT-IR/FIR/NIR Spectrometer Frontier ATR, PerkinElmer, USA) was used to identify the functional groups and the presence of bonds formed in the synthesized powders using different B contents before and after sintering stage. The spectra were recorded in the range of 4000–450 cm^{-1} at 1 cm^{-1} by 20 scans.

To determine the effects of B content and the sintering temperatures on densification behavior and on density, surface of the sintered pellets were observed using FESEM and densities of the sintered pellets were calculated based on their dimensions and weights, respectively.

Vickers microhardness test was conducted on pellets sintered at 1000, 1100 and 1200 °C under 200 g for 15 s after grinding–polishing. Five acceptable hardness measurements were taken on each sample and their arithmetic means and standard deviations were calculated.

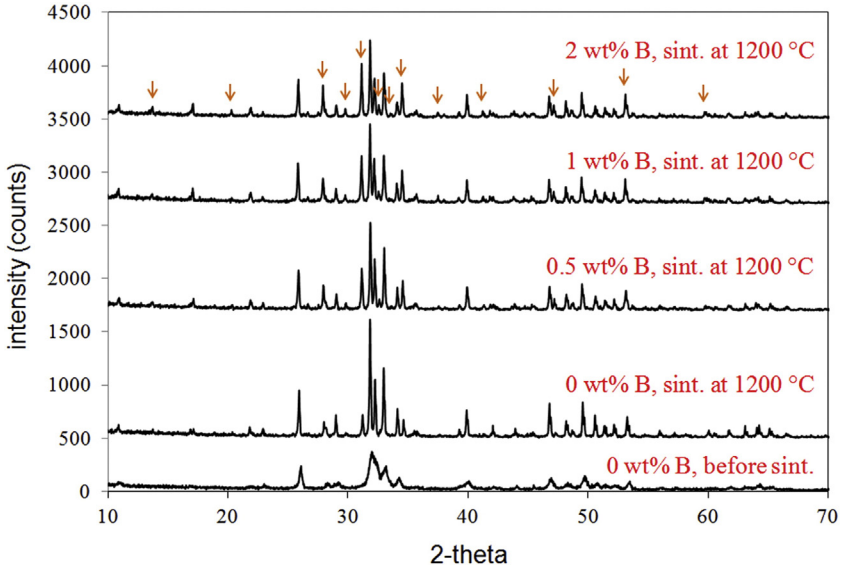

Fig. 3. XRD spectra of the powders synthesized using 0–2 wt.% B (β-TCP peaks are marked).

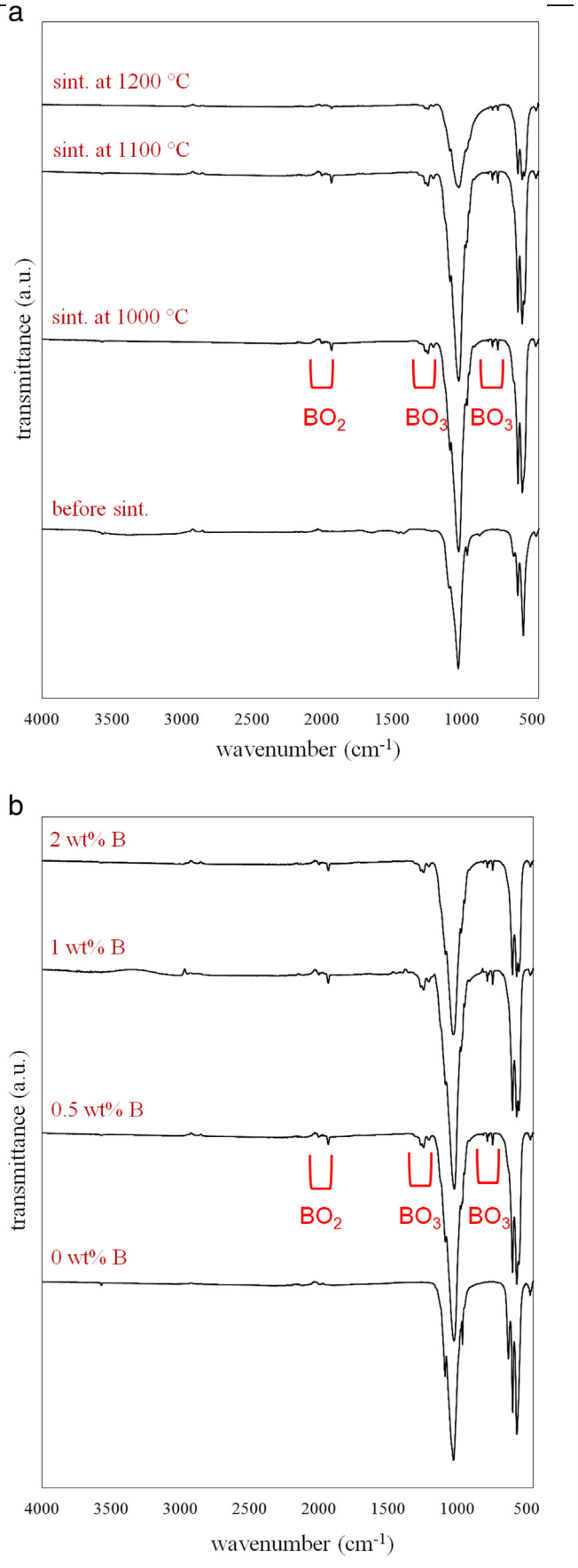

Fig. 4. FTIR spectra of the powders (a) synthesized using 0.5 wt.% B before and after sintering, (b) synthesized using 0–2 wt.% B and sintered at 1100 °C for 2 h.

Table 1
Changes in wt.% values of the phases of undoped and boron doped BCP samples in relation to the sintering temperatures and the boron contents.

Sintering temp.	0 wt.% B (HA/β-TCP)	0.5 wt.% B (BHA/β-TCP)	1 wt.% B (BHA/β-TCP)	2 wt.% B (BHA/β-TCP)
1000 °C	(85.0/15.0)	(76.0/24.0)	(71.9/28.1)	(69.7/30.3)
1100 °C	(83.1/16.9)	(75.2/24.8)	(69.9/30.1)	(65.9/34.1)
1200 °C	(79.0/21.0)	(72.4/27.6)	(67.1/32.9)	(62.2/37.8)

3. Results and discussion

HA powders were produced by acid–base method using various concentrations of boron from 0 wt.% (control sample) to 2 wt.% in the synthesis solution. In order to determine the effects of boron content on the particle size and morphology FESEM images of the synthesized powders were obtained. As seen in Fig. 2a, needle-like particles with approximately 20–40 nm width and 120–150 nm length were synthesized when producing pure HA with no B addition in the synthesis solution. Similar particle size and morphology were obtained even if the boron content was increased to 2 wt.%. Since there was no apparent change in particle size and morphology with varying B content, only the FESEM micrograph of the powders synthesized with the 0.5 wt.% B addition was presented (Fig. 2b).

All of the obtained powders before and after sintering stage were analyzed by XRD to check the phase formation and purity. Before sintering stage, it was determined that XRD peaks of all the synthesized powders (including 0, 0.5, 1 and 2 wt.% B) were completely matched with the HA peaks (PDF Card No: 01-075-9526), no other phases were observed. After sintering stage, XRD spectra and results of phase identification revealed that BCP structure composed of HA and β-TCP (PDF Card No: 01-073-4869) were obtained for all of the samples regardless of the boron content as presented in Fig. 3.

All of the powders synthesized using 0–2 wt.% B were analyzed by FTIR before and after sintering stage at 1000–1200 °C in order to determine the functional groups and to check the formation of boron-related bands, BO_3 and BO_2, in the structure (Fig. 4). The peaks at 962 cm^{-1}, 472 cm^{-1}, 1090 and 1026 cm^{-1}, and 602 and 566 cm^{-1} are attributed to the symmetric stretching v_1, the symmetric bending v_2, the antisymmetric stretching v_3 and the antisymmetric bending v_4 of PO_4^{3-}, respectively [18,32,33]. The peaks at 3570 cm^{-1} and 630 cm^{-1} are attributed

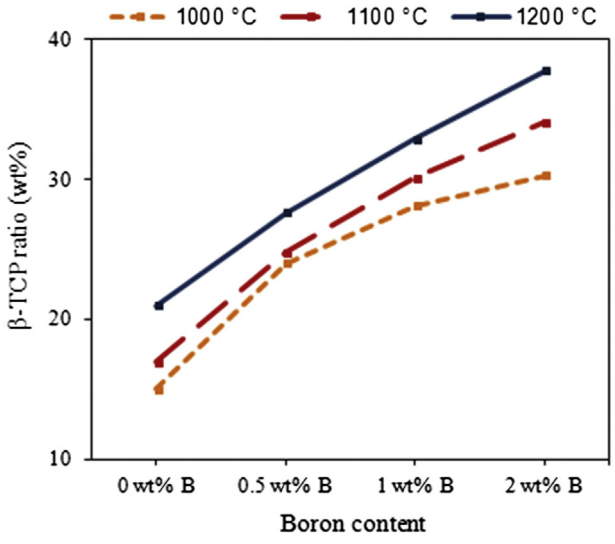

Fig. 5. wt.% of β-TCP in the BCP and boron doped BCP samples, as a function of the boron content and the sintering temperatures.

to the stretching mode ν_S and the librational mode ν_L of OH^-, respectively [18,32]. The bands at 783, 770 and 744 cm^{-1} and 1304, 1253 and 1204 cm^{-1} are attributed to the symmetric bending ν_2 and the antisymmetric stretching ν_3 of BO_3^{3-} groups, respectively [18,22]. The bands at 2002 and 1933 cm^{-1} are attributed to the antisymmetric stretching ν_3 of BO_2^- groups [18,22]. Analysis of the FTIR spectra of the samples synthesized with 0.5 wt.% B addition indicated that although boron related peaks were not observed before the sintering process was applied (Fig. 4a: "before sint." labeled spectrum), these peaks were became apparent after sintering (Fig. 4a: "sint." labeled spectra). This case is valid for all the samples synthesized with different boron contents. As seen in Fig. 4b, the peaks of the BO_3^{3-} and BO_2^- groups are also observed in the FTIR spectra of the sintered powders which were synthesized using 0.5, 1 and 2 wt.% B. It is noticed that sintering stage is required to initiate the chemical reaction between HA and H_3BO_3 as mentioned in [22,23]. The presence of the bands related to the BO_3^{3-} and BO_2^- groups in the FTIR spectra of the sintered samples (Fig. 4) could be the evidence of the boron doping to the HA structure as referred to in [18–20,22].

FTIR analyses revealed that BHA powders would be obtained when the samples synthesized using different boron contents are sintered. Therefore, for these samples the abbreviation BHA would be used instead of HA in the rest of the paper. According to the XRD and FTIR analyses, HA/β-TCP and BHA/β-TCP were obtained after the sintering of the samples synthesized using 0 wt.% B and 0.5–2 wt.% B, respectively. In order to determine the effects of boron content used in the synthesis stage and the sintering temperatures on the wt.% of the phases formed, X-ray powder diffraction software (PDXL 2.1, Rigaku, Japan) mainly based on the Rietveld analysis method was performed. The results obtained (Table 1) indicate that the β-TCP content increases either with the sintering temperature or with the boron amount used in the precipitation stage. As seen in Table 1, β-TCP ratio increases both with the increasing sintering temperature and with the boron content. As the sintering temperature increases from 1000 to 1200 °C, β-TCP ratio increases "from 15.0 to 21.0", "from 24.0 to 27.6", "from 28.1 to 32.9" and "from 30.3 to 37.8" for the samples coded "0 wt.% B", "0.5 wt.% B", "1 wt.% B" and "2 wt.% B", respectively. However, as the boron content increases from 0 wt.% to 2 wt.%, β-TCP ratio increases "from 15.0 to 30.3", "from 16.9 to 34.1" and "from 21.0 to 37.8" for the samples sintered at 1000, 1100 and 1200 °C, respectively. Conclusively, boron content is considered to be more dominant than the sintering temperature on the β-TCP ratio in the final powder. Although the obtained wt.% of β-TCP in the BCP structure is in the range of 15.0 to 21.0, the β-TCP ratio can be increased by sintering at temperatures higher than 1200 °C (Fig. 5). Similarly, the obtained wt.% of β-TCP in the boron doped BCP structure, which is in the range of 24.0 to 37.8, can be altered with modifying the boron content and/or the sintering temperature (Fig. 5).

The densities of the sintered samples were measured and presented in Fig. 6 in order to determine the effects of the boron content used in the synthesis stage and also the sintering temperature. The results indicated that the density of the samples increases with the sintering temperature as expected. The density values of BCP samples composed of HA/β-TCP are increased from 1.54 to 2.71 g/cm^3 with the sintering temperatures as seen in Fig. 6. On the other hand boron content used in the synthesis stage seems to have a negative effect of the densification behavior of the boron doped BCP samples regardless of the sintering temperature and the amount of boron used. As seen in Fig. 6, with the change of the boron content from 0 wt.% to 2 wt.% density values of the samples sintered at 1200 °C decrease from 2.71 to 2.09 g/cm^3. A similar decrease of the density is also observed in the samples sintered at 1000 and 1100 °C. For the boron doped BCP samples the density values changes in the range of 1.39–2.47 g/cm^3 according to the boron content and the sintering temperature. However, the boron content may not be the sole responsible factor for diminishing the density; the ratio of BHA/β-TCP may have some effect on the density changes since the ratio of BHA/β-TCP changes with the boron content and the sintering temperature.

Sinterability of the non-doped and boron doped BCP samples according to the boron content and the sintering temperature was also investigated by the observation of the pore morphology in the FESEM images taken from the sample surfaces (Figs. 7 and 8). The content of the pores decrease as the sintering temperatures increases in all the samples regardless of the boron content as seen in Fig. 7. This result is in agreement with the density evaluations.

FESEM images of the samples with varying boron content revealed that sinterability decreases with increasing boron amount (Fig. 8).

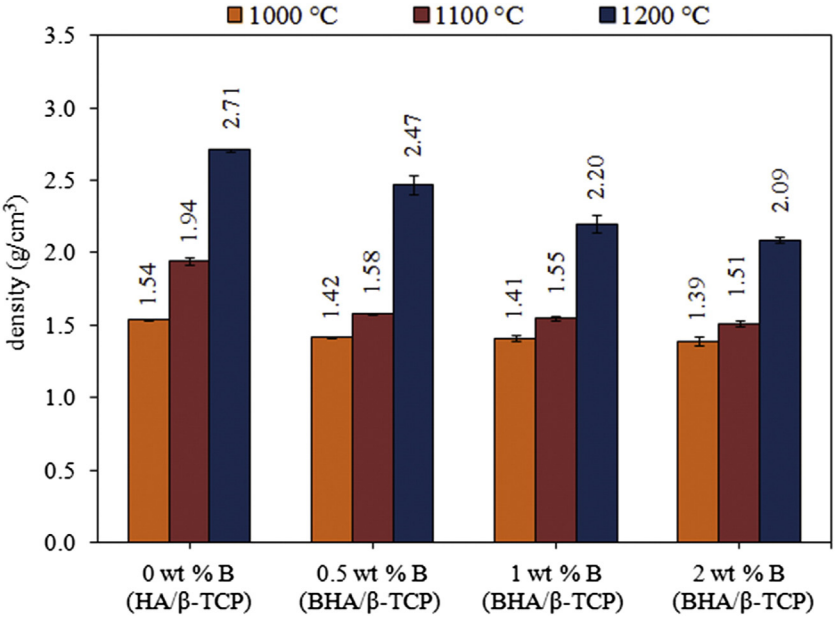

Fig. 6. Density values of the BCP and boron doped BCP samples.

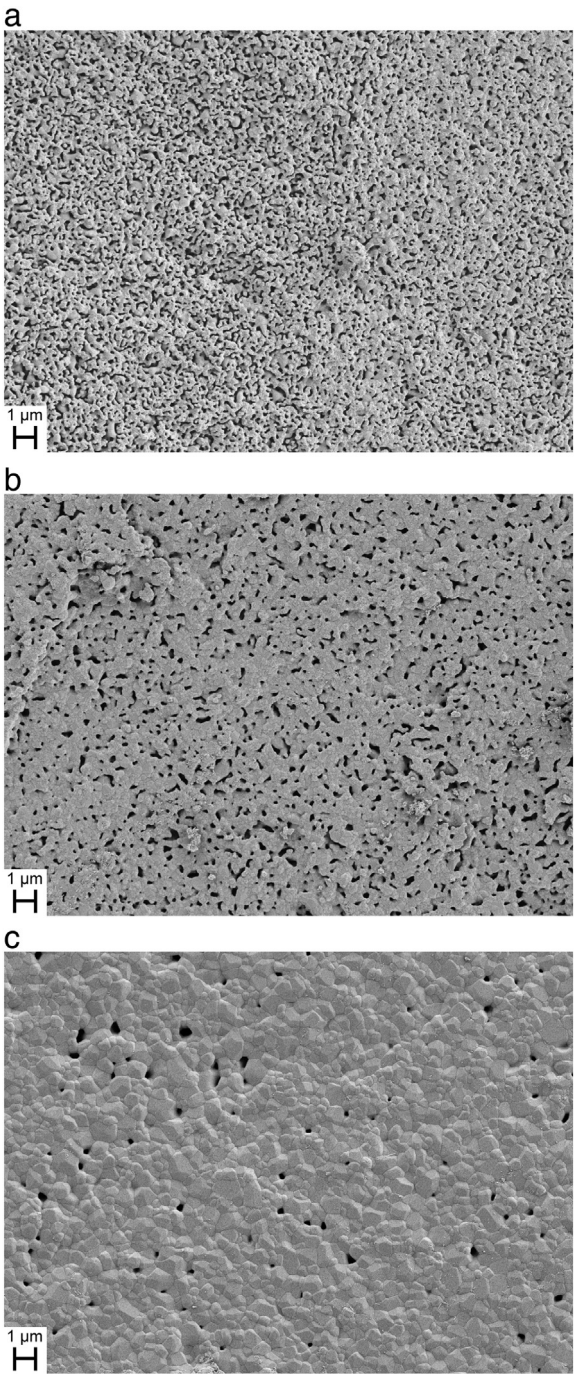

Fig. 7. SEM images of the surfaces of the pellets, which were prepared with the powders synthesized using 1 wt.% B, after sintering at (a) 1000 °C, (b) 1100 °C, (c) 1200 °C for 2 h.

Important to note is that the amount of boron in the BCP structure affect the sinterability of the powder compact negatively. The FESEM images of the uniaxially pressed and sintered samples at 1200 °C presented in Fig. 8 illustrate the relation between the amount of pore and the boron content. Increase in the pore amount in the structure results in the decrease of the sample density which is in agreement with the density evaluations.

Vickers microhardness test was conducted on the pellets, which were prepared using the synthesized powders with different contents of boron as 0, 0.5, 1 and 2 wt.%, and sintered at different temperatures as 1000, 1100 and 1200 °C. Obtained hardness values along with the changes in hardness values with respect to the sintering temperatures and the boron contents were presented in Fig. 9. It can be observed from Fig. 9 that an increase in sintering temperature increases the hardness values of the pellets regardless of the boron content. The significant increase in the hardness values of the samples sintered at 1200 °C is in agreement with the SEM images presented in Fig. 7 in which there is a significant decrease in the pore content. Besides sintering temperature, boron content is responsible for the changes in hardness values, too. As seen in Fig. 9, as the boron content increases from 0 wt.% to 2 wt.% Vickers microhardness values decrease "from 43.27 to 13.59", "from 100.47 to 15.70" and "from 546.30 to 158.36" for the samples sintered at 1000, 1100 and 1200 °C, respectively. The obtained data demonstrate that hardness values decrease with the increasing the boron content.

4. Conclusions

To the best knowledge of the author, the present work is the first study to obtain boron doped biphasic calcium phosphate bioceramics. In this study, undoped and boron doped BCP powders which are composed of HA/β-TCP and BHA/β-TCP, respectively were produced by using the wet precipitation method and then sintering consecutively to obtain varying β-TCP ratios from 15.0 to 37.8 wt.%.

The effects of the boron content used in the precipitation stage and the effects of sintering temperature on the structure, β-TCP ratio, densification, sinterability and microhardness can be summarized as follows:

- The morphological features of the synthesized powders have not shown obvious differences between boron doped and undoped samples. All particles are needle-like with approximately 20–40 nm in width and 120–150 nm in length regardless of the amount of boron added.
- XRD and FTIR analyses before sintering stage revealed that all of the synthesized powders (nondoped and 0.5–2 wt.% B doped) completely matched with HA; no other peaks were detected.
- XRD spectra and results of phase identification after sintering stage revealed that BCP structure composed of HA and β-TCP were obtained for all the samples regardless of the boron content.
- After sintering stage the presence of the bands related to the BO_3^{3-} and BO_2^- groups in the FTIR spectra of the samples synthesized using different amounts of boron reveals that boron doped HA powders were obtained.
- Evaluation of the XRD and FTIR analyses revealed that BCP (HA/β-TCP) and boron doped BCP (BHA/β-TCP) were obtained after sintering stage for the samples synthesized using 0 wt.% B and 0.5–2 wt.% B, respectively.
- Boron doping enhances the decomposition of HA into β-TCP. The β-TCP ratio in undoped and boron doped BCP varies in the range of 15.0–21.0 wt.% and 24.0–37.8 wt.%, respectively according to the boron content used in the synthesis stage and the sintering temperature.
- wt.% of β-TCP in both the undoped and boron doped BCP structures increase with either the sintering temperature or the boron content used in the precipitation stage. Desired β-TCP ratio in the range limit could be obtained with modifying the boron content used in the synthesis stage and the sintering temperature.
- Unlike the sintering temperature, boron content used in the synthesis stage has a negative effect on the densification, sinterability and microhardness of the boron doped BCP samples. As the boron content increases, densification, sinterability and microhardness deteriorate.
- Desired values of density and microhardness within a specified range can be obtained with modifying the boron content used in the synthesis stage and the sintering temperature.

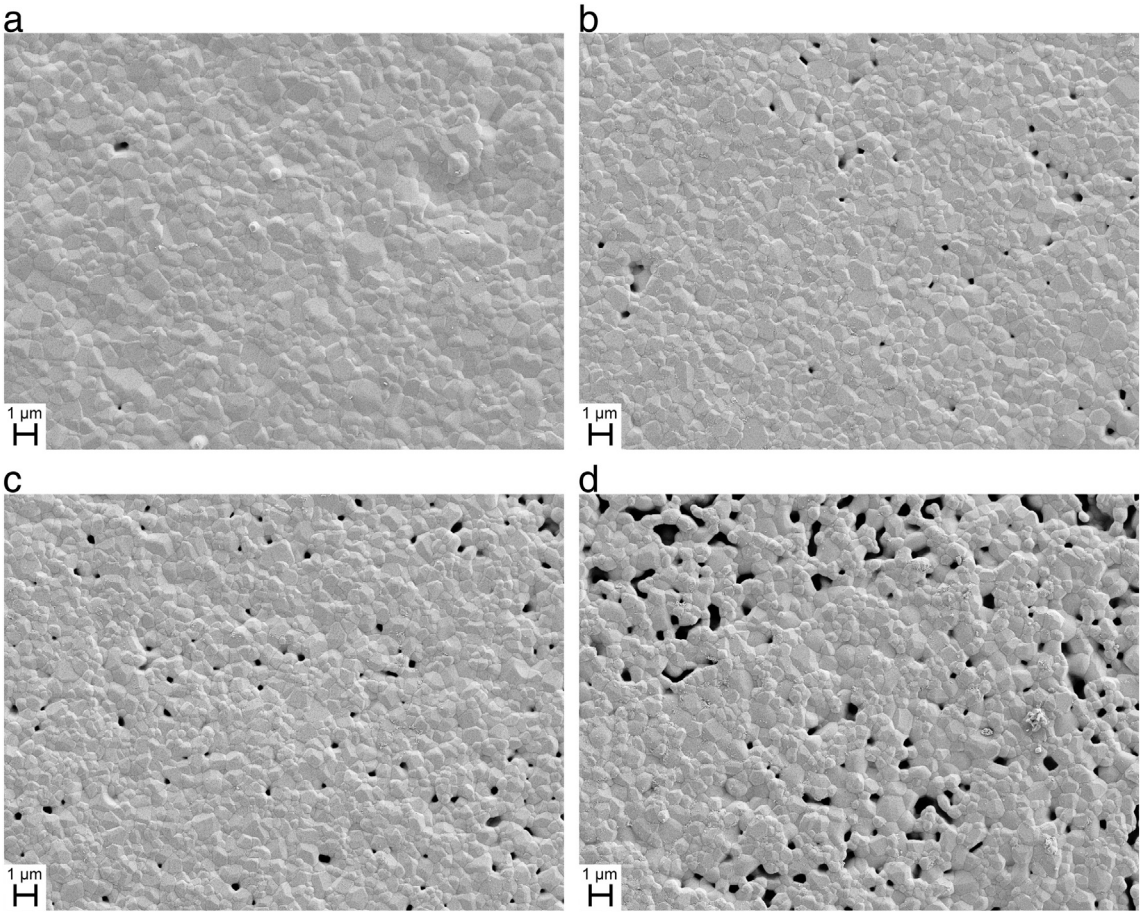

Fig. 8. SEM images of the surfaces of the pellets, which were prepared with the powders synthesized using (a) 0 wt.% B, (b) 0.5 wt.% B, (c) 1 wt.% B, (d) 2 wt.% B, after sintered at 1200 °C for 2 h.

Acknowledgments

This work was supported in part by The Scientific and Technological Research Council of Turkey (TUBITAK) with the project number 213M621. The author would also like to thank Mustafa Ugurlu who worked as a student scholarship in the project 213M621 and to "Mersin University Advanced Technology, Training, Research and Application

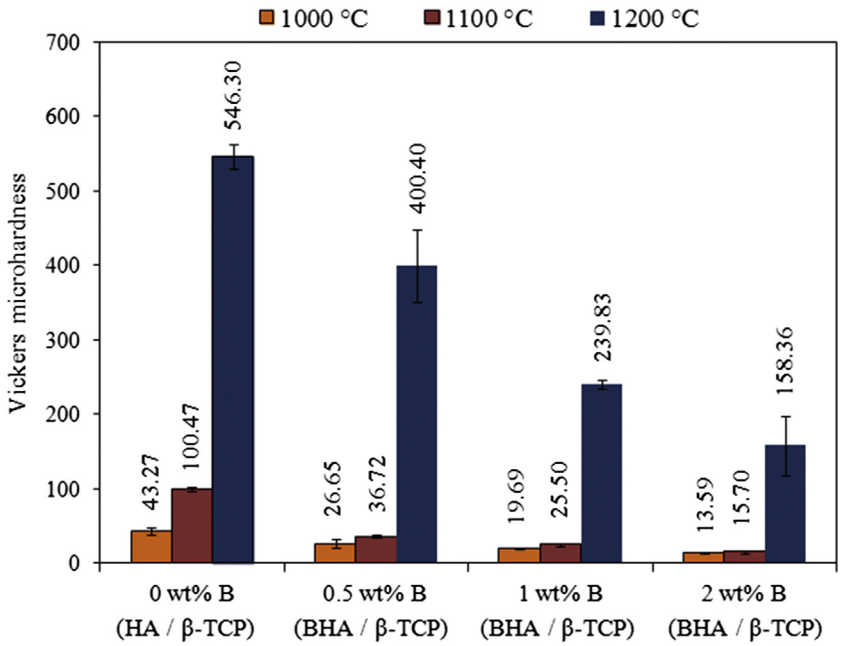

Fig. 9. Microhardness values of the BCP and boron doped BCP samples, as a function of the boron content and the sintering temperatures.

Center" (MEITAM) for the opportunity of using the SEM, XRD and FT-IR equipment.

References

[1] B. Liu, D.X. Lun, Current application of β-tricalcium phosphate composites in orthopaedics, Orthop. Surg. 4 (2012) 139–144.
[2] O. Albayrak, S. Altintas, Production of 'tricalcium phosphate/titanium dioxide' coating surface on titanium substrates, J. Mater. Sci. Technol. 26 (2010) 1006–1010.
[3] K.P. Sanosh, M.C. Chu, A. Balakrishnan, T.N. Kim, S.J. Cho, Preparation and characterization of nano-hydroxyapatite powder using sol–gel technique, Bull. Mater. Sci. 32 (2009) 465–470.
[4] H. Valiense, M. Barreto, R.F. Resende, A.T. Alves, A.M. Rossi, E. Mavropoulos, J.M. Granjeiro, M.D. Calasans-Maia, In vitro and in vivo evaluation of strontium-containing nanostructured carbonated hydroxyapatite/sodium alginate for sinus lift in rabbits, J. Biomed. Mater. Res. (2015) http://dx.doi.org/10.1002/jbm.b.33392.
[5] M. Hirota, Y. Matsui, N. Mizuki, T. Kishi, K. Watanuki, T. Ozawa, T. Fukui, S. Shoji, M. Adachi, Y. Monden, T. Iwai, I. Tohnai, Combination with allogenic bone reduces early absorption of β-tricalcium phosphate (β-TCP) and enhances the role as a bone regeneration scaffold. Experimental animal study in rat mandibular bone defects, Dent. Mater. J. 28 (2009) 153–161.
[6] S. Bansal, V. Chauhan, S. Sharma, R. Maheshwari, A. Juyal, S. Raqhuvanshi, Evaluation of hydroxyapatite and beta-tricalcium phosphate mixed with bone marrow aspirate as a bone graft substitute for posterolateral spinal fusion, Indian J. Orthop. 43 (2009) 234–239.
[7] H.R.R. Ramay, M. Zhang, Biphasic calcium phosphate nanocomposite porous scaffolds for load-bearing bone tissue engineering, Biomaterials 25 (2004) 5171–5180.
[8] N.C. Bleach, S.N. Nazhat, K.E. Tanner, M. Kellomaki, P. Tormala, Effect of filler content on mechanical and dynamic mechanical properties of particulate biphasic calcium phosphate–polylactide composites, Biomaterials 23 (2002) 1579–1585.
[9] G. Daculsi, O. Laboux, O. Malard, P. Weiss, Current state of the art of biphasic calcium phosphate bioceramics, J. Mater. Sci. Mater. Med. 14 (2003) 195–200.
[10] S.H. Kwon, Y.K. Jun, S.H. Hong, H.E. Kim, Synthesis and dissolution behavior of β-TCP and HA/β-TCP composite powders, J. Eur. Ceram. Soc. 23 (2003) 1039–1045.
[11] G. Daculsi, Biphasic calcium phosphate concept applied to artificial bone, implant coating and injectable bone substitute, Biomaterials 19 (1998) 1473–1478.
[12] T.W. Kim, Y. Min Park, D.H. Kim, H.H. Jin, K.K. Shin, J. Sup Jung, H.C. Park, S.Y. Yoon, In situ formation of biphasic calcium phosphates and their biological performance in vivo, Ceram. Int. 38 (2012) 1965–1974.
[13] R.H. Jain, J.Y. Marzillier, T.J. Kowal, S. Wang, H. Jain, M.M. Falk, Expression of mineralized tissue-associated proteins is highly upregulated in MC3T3-E1 osteoblasts grown on a borosilicate glass substrate, in: R. Narayan, P. Colombo, S. Widjaja, D. Singh (Eds.), Ceramic Engineering and Science Proceedings: Advances in Bioceramics and Porous Ceramics IV, vol. 32, John Wiley & Sons Inc., New Jersey 2011, pp. 111–119.
[14] S.S. Hakki, B.S. Bozkurt, E.E. Hakki, Boron regulates mineralized tissue-associated proteins in osteoblasts (MC3T3-E1), J. Trace Elem. Med. Biol. 24 (2010) 243–250.
[15] A.A. Gorustovich, J.M.P. Lopez, M.B. Guglielmotti, R.L. Cabrini, Biological performance of boron-modified bioactive glass particles implanted in rat tibia bone marrow, Biomed. Mater. 1 (2006) 100–105.
[16] X. Xue, Y. Wang, H. Yang, Preparation and characterization of boron-doped titania nano-materials with antibacterial activity, Appl. Surf. Sci. 264 (2013) 94–99.
[17] Y. Wang, X. Xue, H. Yang, Preparation and characterization of carbon or/and boron-doped titania nano-materials with antibacterial activity, Ceram. Int. 40 (2014) 12533–12537.
[18] R. Ternane, M.T. Cohen-Adad, G. Panczer, C. Goutaudier, N. Kbir-Ariguib, M. Trabelsi-Ayedi, P. Florian, D. Massiot, Introduction of boron in hydroxyapatite: synthesis and structural characterization, J. Alloys Compd. 333 (2002) 62–71.
[19] S. Barheine, S. Hayakawa, C. Jager, Y. Shirosaki, A. Osaka, Effect of disordered structure of boron-containing calcium phosphates on their in vitro biodegradability, J. Am. Ceram. Soc. 94 (2011) 2656–2662.
[20] A. Ito, H. Aoki, M. Akao, N. Miura, R. Otsuka, S. Tsutsumi, Structure of borate groups in boron-containing apatite, J. Ceram. Soc. Jpn. 96 (1988) 707–709.
[21] S. Barheine, S. Hayakawa, A. Osaka, C. Jaeger, Surface, interface, and bulk structure of borate containing apatitic biomaterials, Chem. Mater. 21 (2009) 3102–3109.
[22] H. Guler, G. Gundogmaz, F. Kurtulus, G. Celik, S.S. Gacanoglu, Solid state synthesis of calcium borohydroxyapatite, Solid State Sci. 13 (2011) 1916–1920.
[23] S. Hayakawa, A. Sakai, K. Tsuru, A. Osaka, E. Fujii, K. Kawabata, C. Jager, Preparation and characterization of boron-containing hydroxyapatite, Key Eng. Mater. 361-363 (2008) 191–194.
[24] O. Albayrak, O. El-Atwani, S. Altintas, Hydroxyapatite coating on titanium substrates by electrophoretic deposition method: effects of titanium dioxide inner layer on adhesion strength and hydroxyapatite decomposition, Surf. Coat. Technol. 202 (2008) 2482–2487.
[25] M. Wei, Electrophoresis of Hydroxyapatite on Metal Substrates(PhD Thesis) University of New South Wales, 1997.
[26] H. Tagai, H. Aoki, Preparation of synthetic hydroxyapatite and sintering of apatite ceramics, in: G.W. Hastings, D.F. Williams (Eds.), in Mechanical Properties of Biomaterials, John Wiley and Sons, New York 1980, pp. 477–488.
[27] P.N. Kumta, C. Sfeir, D.-H. Lee, D. Olton, D. Choi, Nanostructured calcium phosphates for biomedical applications: novel synthesis and characterization, Acta Biomater. 1 (2005) 65–83.
[28] M. Ansari, S.M. Naghib, F. Moztarzadeh, A. Salati, Synthesis and characterization of hydroxyapatite calcium hydroxyapatite for dental composites, Ceramics-Silikáty 55 (2) (2011) 123–126.
[29] D.C. Tancred, A.J. Carr, B.A.O. Mccormack, The sintering and mechanical behavior of hydroxyapatite with bioglass addition, J. Mater. Sci. Mater. Med. 12 (2001) 81–93.
[30] J.F. Gomes, C.C. Granadeiro, M.A. Silva, M. Hoyos, R. Silva, T. Vieira, An investigation of the synthesis parameters of the reaction of hydroxyapatite precipitation in aqueous media, Int. J. Chem. React. Eng. 6 (2008) 1–15, A103.
[31] Rigaku Corporation, Integrated X-ray Powder Diffraction Software PDXL 2.1: Rietveld Analysis User Manual, Rigaku Corporation, Tokyo, 2012.
[32] H. Ye, X.Y. Liu, H. Hong, Characterization of sintered titanium/hydroxyapatite biocomposite using FTIR spectroscopy, J. Mater. Sci. Mater. Med. 20 (2009) 843–850.
[33] O. Albayrak, M. Ipekoglu, N. Mahmutyazicioglu, M. Varmis, E. Kaya, S. Altintas, Preparation and characterization of porous hydroxyapatite pellets: effects of calcination and sintering on the porous structure and mechanical properties, Proc. Inst. Mech. Eng. L J. Mater. Des. Applic. (2015) http://dx.doi.org/10.1177/1464420715591859.